JOURNAL OF CATALYSIS **162,** 368–376 (1996)
ARTICLE NO. 0296

ERRATUM

Volume **160**, Number 1 (1996), in the article "Investigation of V Oxidation States in Reduced V/Al_2O_3 Catalysts by XPS," by Mary A. Eberhardt, Andrew Proctor, Marwan Houalla, and David M. Hercules, pages 27–34: Due to a printer's error, Figures 1, 2, 3, 4, 5, 6, 7, and 8 were printed at incorrect resolution. For the reader's convenience, the entire article is reprinted here.

JOURNAL OF CATALYSIS **160,** 27–34 (1996)
ARTICLE NO. 0120

Investigation of V Oxidation States in Reduced V/Al_2O_3 Catalysts by XPS

Mary A. Eberhardt, Andrew Proctor, Marwan Houalla, and David M. Hercules

Department of Chemistry and Materials Research Center, University of Pittsburgh, Pittsburgh, Pennsylvania 15260

Received August 9, 1994; revised April 27, 1995

The distribution of vanadium oxidation states in a 5.9 wt% V/Al_2O_3 catalyst reduced in H_2 or CO was determined from XPS V 2*p* spectra. Principal component analysis (PCA) was used to statistically determine the number of components (oxidation states) that describe the V $2p_{3/2}$ envelope of the reduced V/Al_2O_3 catalyst. The peak positions and FWHMs of the components were obtained from iterative target transformation factor analysis (ITTFA). The V $2p_{3/2}$ envelope is composed of two components (oxidation states), which are centered at 517.2 and 515.5 eV (FWHMs of 2.6 and 2.3 eV, respectively) when H_2 is the reducing agent and at 517.3 and 515.8 eV (FWHMs 2.7–2.8 eV) when CO is the reducing agent. The components were assigned to V^{5+} and V^{3+} based on the difference in the binding energies and the results of a volumetric study of catalyst reduction in CO. The spectral information gained from PCA and ITTFA was used to curve fit the V 2*p* envelopes. The extent of reduction of the V phase was estimated from the relative abundances of V^{5+} and V^{3+} determined by curve fitting and corrected for the presumably lower dispersion of the V^{3+} species. The results indicated a decrease in the average oxidation state of V to 3.5 with increasing the reduction temperature in H_2 up to 662°C. Reduction in the presence of CO was measured volumetrically and showed a decrease in the average oxidation state from 5 to 3.3 over the temperature range 155–510°C. Curve fitting the spectra of the CO-reduced samples using the two spectral components identified through factor analysis yielded an average oxidation state of ca. 3.6 upon reduction at 510°C. © 1996 Academic Press, Inc.

INTRODUCTION

Vanadium catalysts are currently the subject of much research due to their high activity in the reduction of NO by ammonia to N_2 and O_2 (1–3). Bulk and supported vanadium catalysts are also active in selective oxidation reactions (4–6). The activation of vanadium catalysts often involves a reduction pretreatment, which may lead to the formation of a mixture of vanadium oxidation states. Since the extent of reduction affects the activity (5, 6) it is desirable to know the distribution of vanadium oxidation states.

To date, most methods used to monitor the reduction of supported vanadium catalysts can only measure the average oxidation state (7–11). A recent temperature-programmed reduction (TPR) study has shown that V/Al_2O_3 catalysts reduced to an average oxidation state of 4 (7), while other researchers have measured an average oxidation state of 3 by TPR for similar catalysts (8). The latter TPR study (8) was in variance with the results of gravimetric analysis in which an average oxidation state of 4 was reported (9–11). The discrepancy between TPR and gravimetric studies has been addressed in the literature (9). Clearly, there is a need for a technique capable of measuring the distribution of V oxidation states. Electron spin resonance (ESR) has been used to study the reduction of supported vanadium catalysts (1, 12–16). However, the technique, by definition, can only monitor paramagnetic species (V^{4+}).

In principle, X-ray photoelectron spectroscopy (XPS) should be an effective technique for monitoring the distribution of vanadium oxidation states because of the large V 2*p* binding energy difference between V^{5+} and V metal (ca. 4.5 eV) (17). Indeed, XPS has been used extensively to examine vanadium oxides and supported V catalysts (17–30). However, results of these studies were often inconclusive. The reported binding energies of model V compounds vary by as much as 2.5 eV between research groups for a given oxidation state (20). The discrepancies in the literature can be partially attributed to the difficulty in analyzing the XPS V 2*p* region due to its overlap with the O 1*s* peak (ca. 531 eV) and the O 1*s* X-ray-induced satellites in nonmonochromatic spectrometers. In addition, in the case of supported catalysts such as V/Al_2O_3, the O 1*s* signal is predominant and can obscure small binding energy shifts of the V 2*p* signal. The overlap between the XPS V 2*p* region and the O 1*s* X-ray-induced satellites can be addressed since the X-ray spectrum of Al, the X-ray source in the spectrometer, is well known and thus, the O 1*s* X-ray-induced satellites can be subtracted from the spectrum, leaving the V 2*p* peaks. An added difficulty in previous XPS studies is the need to curve fit the V $2p_{3/2}$ region when more than one oxidation state is present (11, 26, 30). Nonlinear least-squares curve fitting (NLLSCF) is commonly used to fit peaks into a given XPS envelope (31) and to determine the distribution of oxidation states. However, curve fitting requires the users to make assumptions concerning the number of peaks under a

0021-9517/96 $18.00

given envelope and their characteristics (position, FWHM, shape). The lack of reliable binding energy positions for V oxidation states and the uncertainty in the number of oxidation states present in reduced catalysts preclude curve fitting the XPS V 2*p* envelope with confidence. This highlights the need to employ independent methods for identifying the number and positions of V oxidation states present in reduced catalysts.

We have shown in the case of Mo/TiO_2 catalysts that principal component analysis (PCA) can be used to statistically determine the number of components that compose an XPS envelope (32). Peak positions and FWHMs could be obtained from iterative target transformation factor analysis (ITTFA). These parameters, derived without assumptions concerning the number, position, and shape of the peaks, could then be used in NLLSCF to obtain the distribution of components in a series of reduced catalysts.

The present study will apply the above-mentioned methodology for analysis of XPS spectra to monitor the reduction of an alumina-supported V catalyst. The XPS spectra will be analyzed by factor analysis (FA), consisting of PCA and ITTFA, to determine the number and positions of components, or oxidation states, present in a series of reduced V/Al_2O_3 catalysts. The information obtained from factor analysis is used to curve fit the V 2*p* spectra. The distribution of the vanadium oxidation states is used to calculate the average oxidation state for comparison with volumetric studies.

EXPERIMENTAL

Catalyst Preparation

The catalyst was prepared using a 0.05*M* solution of NH_4VO_3. γ-Alumina (Cyanamid, 175 m^2/g, 100 mesh) was added to the vanadium solution and the pH of preparation was adjusted to 5.0 using 4*M* HNO_3 and NH_4OH solutions. The pH was periodically adjusted as necessary to maintain pH 5 throughout the 24-hr mixing time. The catalyst was filtered, dried at 120°C for 4 hr, and calcined in a dry air flow at 500°C for 16 hr. The resulting catalyst contained 5.9 wt% V, determined by X-ray fluorescence. This vanadium loading was chosen because it is well below the loading required for full monolayer coverage of the support (12.6 wt% V) (8).

Catalyst Treatment

The V/Al_2O_3 catalyst, pressed (2 tons) into a pellet, was mounted on a sealable probe and heated at 2°C/min to the desired reduction temperature. The catalyst was reduced in UHP H_2 (ca. 90 cm^3/min) for 8 hr and then cooled to room temperature. The probe was sealed under 25 psi UHP H_2 and transferred to the spectrometer without exposure to air.

Stoichiometric Measurements

Stoichiometric measurements were performed using a conventional BET system, modified to include a glass circulating loop. The powdered catalyst (ca. 0.5 g) was oxidized in flowing 10% O_2/He at 450°C for 4 hr, cooled to room temperature, and evacuated for 16 hr. The catalyst was reduced in the circulating loop of the BET system using ca. 270 mbar (1 bar = 10^5 N/m^2) CO at the desired temperature, until there was no significant change in the CO consumption (ca. 8 hr). CO_2 produced upon reduction was collected using a liquid N_2-cooled trap, and the CO consumed was measured manometrically. The sample was then reoxidized at 450°C in 270 mbar O_2 and the O_2 consumption was measured. This procedure yielded three measures of the average oxidation state of V.

The catalyst reduced in the volumetric system was transferred to a glovebox, pressed into a pellet, and mounted on a sealable probe. This allowed XPS analysis of the catalyst after reduction treatment in the volumetric system without exposing the sample to air. In this manner the average oxidation state measured stoichiometrically could be compared with the distribution of the V oxidation states determined from XPS.

X-Ray Photoelectron Spectroscopy

XPS spectra were collected using a modified AEI ES200A electron spectrometer equipped with an Al anode (Al $K\alpha = 1486.6$ eV) operated at 12 kV and 20 mA. The base pressure in the analysis chamber was below 10^{-8} mbar. All XPS binding energies are referenced to the Al 2*p* peak of γ-Al_2O_3 at 74.5 eV. The intrinsic resolution of the spectrometer (FWHM) was observed to be 1.6 eV for Au $4f_{7/2}$ (84.0 eV). The data collection was controlled by an IBM compatible PC interfaced with the spectrometer. Data acquisition time was minimized to avoid reducing the vanadium in the spectrometer by prolonged exposure to X rays (19).

We have observed up to 50% decrease in the XPS V/Al ratio as the V/Al_2O_3 catalyst is reduced, indicating sintering of the V surface phase. As shown earlier, this could lead to an underestimation of the extent of reduction obtained from simply curve fitting the V 2*p* envelope of the reduced catalyst (33). The extent of reduction was thus calculated from the V 2*p* spectra using the modified XPS method (33). It is assumed that the unreduced phase is atomically dispersed. The fraction of V unreduced, $[V]_{unred}$, is calculated as

$$[V]_{unred} = (I_M)_{unred}/(I_M)_{mono}, \quad [1]$$

where $(I_M)_{unred}$ is the V $2p_{3/2}$/Al 2*p* intensity ratio of the unreduced part of the V 2*p* spectrum after CO or H_2 reduction treatment, and $(I_M)_{mono}$ is the predicted V/A1 intensity ratio based on a monolayer dispersion of the V phase

(34). The fraction of vanadium reduced to a lower oxidation state, $[V]_{red}$, will then equal

$$[V]_{red} = 1 - [V]_{unred}. \quad [2]$$

Data Analysis

The theoretical considerations of FA for XPS spectra have been described in detail previously (32, 35), In the present study principal component analysis was utilized to determine the number of components, *n* (oxidation states) present in V 2*p* spectra of reduced V/Al_2O_3 catalysts. A uniqueness test (36, 37) was performed on the data matrix of spectra. The uniqueness test indicates spectra that are atypical of the series of spectra due to unique properties or errors in the data. Statistical tests were used to determine which components of the data matrix represent noise and which represent signal. The IND function, an empirical measure of Malinowski (36), will minimize at the correct number of signal components. The *Q*% is used to distinguish between factors that are noise and those that are signal (37). A *Q*% value greater than 10% has been shown to indicate noise (32, 35). The last statistical test used to evaluate the data matrix is the reduced eigenvalue ratio (REV ratio). The REV ratio will be close to unity when two error eigenvalues are compared and significantly greater than unity when an eigenvalue containing a signal (component) is encountered.

The positions of the spectral components can be obtained by performing a "needle" search using the *n* factors (components) found by PCA (32). The real component locations on the abscissa are probed using a very narrow test spectrum, a delta function, which has a value of zero at all points except one, where it is unity. Each spectrum contains *N* points; therefore, *N* tests with *N* delta functions are performed to produce *N* separate predicted spectra. In this manner the positions of *n* spectral components are indicated at the points where the predicted spectra most closely match the test spectra. Iterative target transformation is then carried out using initial delta functions at these positions, which produce predicted spectral components that are then modified and used as the test data for the next iteration. When the test data match the predicted data closely the resultant spectra should represent the pure spectral components.

Curve fitting was performed on the V $2p_{3/2}$ region using a Levenberg–Marquardt NLLSCF routine and information obtained from factor analysis (number of components, positions, and FWHM). The O 1*s* peak was first curve fitted, and then the related X-ray-induced satellite peaks were subtracted, leaving the V $2p_{3/2}$ and V $2p_{1/2}$ envelope.

RESULTS

XPS spectra of the V $2p_{3/2}$ region, after subtraction of the X-ray-induced satellites of O 1*s* peak, are shown in Figs. 1

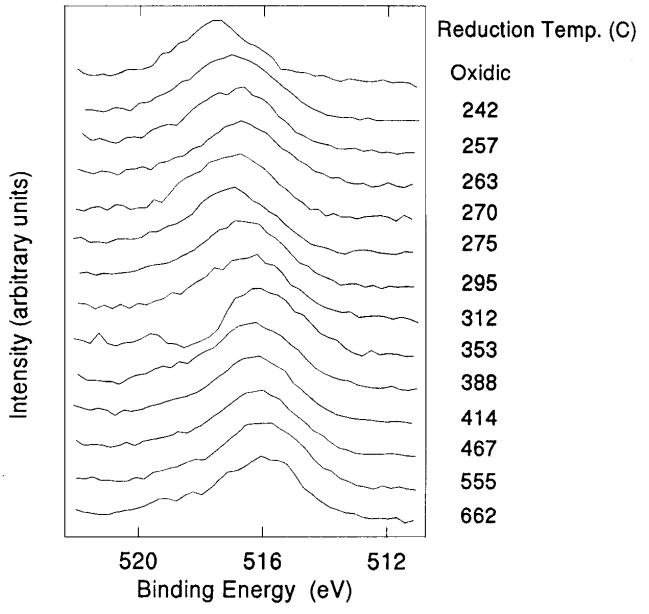

FIG. 1. V $2p_{3/2}$ spectra after removing the O 1*s* peak and X-ray-induced satellite for V/Al_2O_3 catalyst reduced in H_2 at the indicated temperatures.

and 2 for 5.9 wt% V/Al_2O_3 reduced in H_2 and CO, respectively. It is clear that the position of the V $2p_{3/2}$ peak shifts toward lower binding energy as the reduction temperature increases, but the number of peaks that contribute to the envelopes is difficult to ascertain. The uniqueness test was

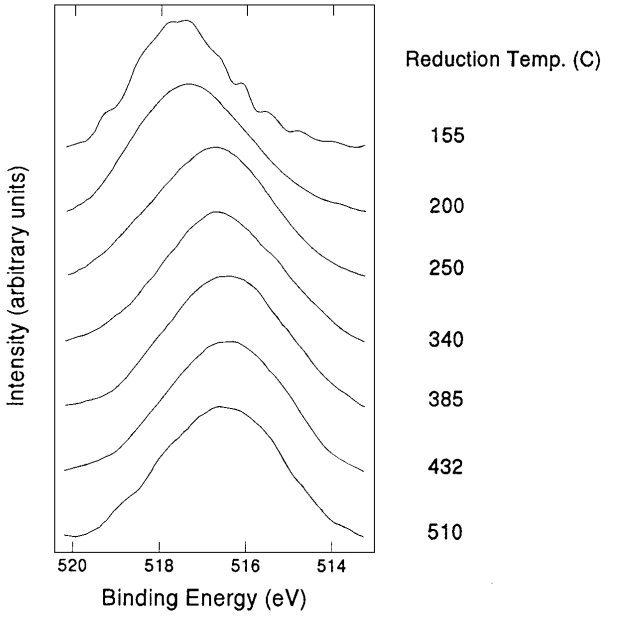

FIG. 2. V $2p_{3/2}$ spectra after removing the O 1*s* peak and X-ray-induced satellite for V/Al_2O_3 catalyst reduced in CO at the indicated temperatures. The spectra were smoothed using a Savitsky–Golay function.

TABLE 1

Statistical Tests for PCA of 10 Spectra of 5.9 wt% V/Al_2O_3 Reduced in H_2

Factor	REV Ratio	IND	Q (%)
1	40.2382	0.9767E−3	0.3723E−4
2	**16.0409**	**0.4925E−3**	**0.1200**
3	1.22000	0.5605E−3	22.818
4	1.44379	0.6588E−3	24.358
5	1.07613	0.8485E−3	31.668
6	1.33219	0.1162E−2	32.736
7	1.24601	0.1882E−2	41.441
8	0.552889	0.4159E−2	53.310
9	1.02567	0.1344E−2	49.596
10	1.00000	0.0000	0.0000

performed on the spectra in Fig. 1 to identify those that are atypical of the whole series. The spectra of the oxidic catalyst and the catalyst reduced at 270, 275, and 353°C were identified as unique spectra and removed from the series. In previous studies we have shown that removing the spectrum of the oxidic sample from the data matrix improves the statistical measure of the number of components found in PCA (32). While the anomalous peak shape in the spectrum for the 353°C H_2 reduction is obvious, the rejection of the spectra of samples reduced at 270 and 275°C can be due, in part, to artifacts of subtracting the O 1*s* X-ray-induced satellite peaks. The remaining 10 spectra were smoothed and used in the data matrix analyzed by PCA.

PCA results are given in Table 1 for the data matrix of spectra of H_2-reduced samples. The IND function minimizes at factor 2, the Q% decreases dramatically from factor 3 to factor 2 (using a cutoff of 10% for real signal), and the REV ratio increases from 1.22 to 16.0 between factors 3 and 2. The IND, REV Ratio, and Q% all indicate the presence of two factors. The results of PCA performed on the matrix of spectra from CO-reduced samples (Fig. 2) are given in Table 2. It is clear that two factors are found by PCA; i.e., the IND function minimizes at two factors, the Q% decreases from 18 to $\ll 1$ when one compares factor 3 to factor 2, and the REV ratio increases from 2.0 to 67 between factors 3 and 2.

TABLE 2

Statistical Tests for PCA of Seven Spectra of 5.9 wt% V/Al_2O_3 Reduced in CO

Factor	REV Ratio	IND	Q (%)
1	21.8244	0.3376E−2	0.1372E−1
2	**67.0055**	**0.7735E−3**	**0.1256E−1**
3	2.05586	0.8839E−3	18.035
4	1.71980	0.1263E−2	29.848
5	0.84278	0.2556E−2	45.549
6	1.00036	0.8324E−2	49.994
7	1.00000	0.0000	0.0000

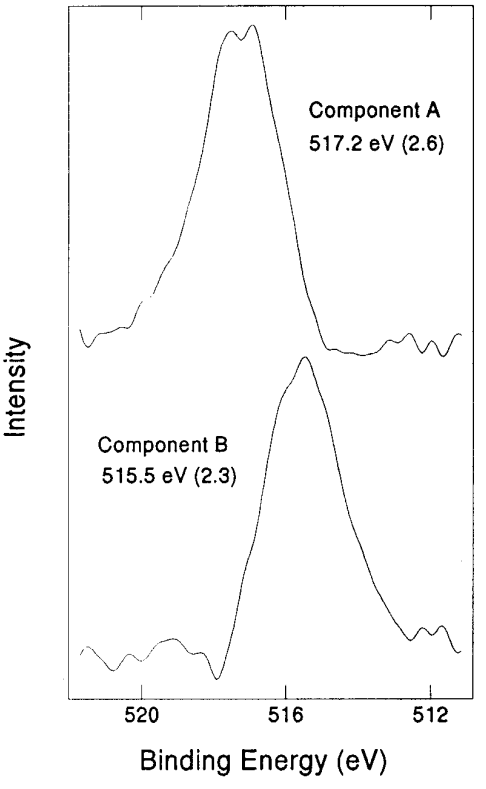

FIG. 3. Spectral components generated by ITTFA for H_2 reduction. The FWHM is given in parentheses.

ITTFA was used to generate two spectral components at positions indicated by the needle search. From these we obtain the binding energies and approximate FWHMs of the spectral components. Figure 3 shows the two components derived through ITTFA for the H_2-reduced series. It should be noted that the peaks produced in ITTFA *do* resemble real XPS peaks although no peak shape information was included in the transformation procedure. The peaks are centered at 517.2 eV (Component A) and 515.5 eV (Component B) with FWHMs of 2.6 and 2.3 eV, respectively. ITTFA was also performed on the spectra of CO-reduced series. The components generated from ITTFA are shown in Fig. 4. The peaks are centered at 517.3 eV (Component A) and 515.8 eV (Component C), with FWHMs of 2.7–2.8 eV, which are slightly larger than those measured for the H_2-reduced series.

The number of components, peak positions, and FWHMs found by factor analysis were then used to curve fit the V $2p_{3/2}$ spectra after subtraction of the O 1*s* peak and smoothing using a cubic spline (38). Figure 5 shows spectra of oxidic V/Al_2O_3 and the catalyst reduced in H_2 at 312°C, curve fitted using the parameters found by FA. The peak positions and FWHMs were allowed to vary by ± 0.2 eV to

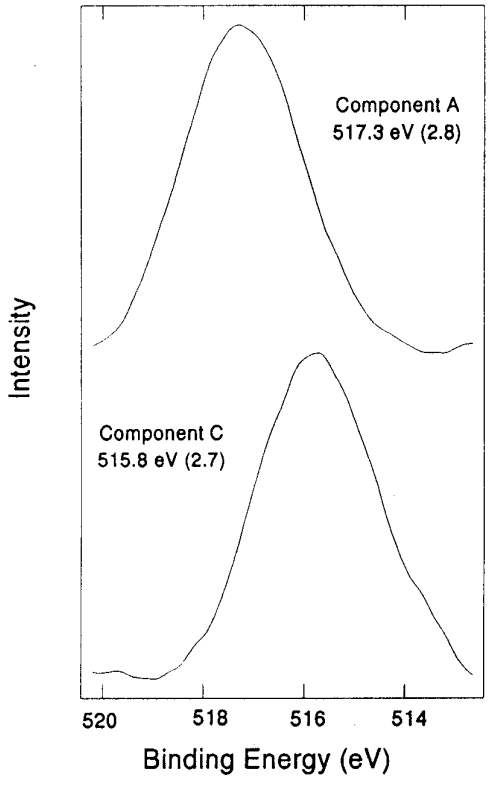

FIG. 4. Spectral components generated by ITTFA for CO reduction. The FWHM is given in parentheses.

relax into their local minima. Note that curve fitting the V 2*p* spectrum of the oxidic catalyst shows a small amount of Component B (ca. 13%). The sample was pretreated in 10% O_2/He at 450°C, which should fully oxidize the vanadium. It is probable that the slight reduction observed is occurring in the XPS chamber from stray electrons (25).

The distribution of components is plotted as a function of the reduction temperature in Fig. 6 for samples reduced in H_2. The relative abundance of Component A decreases from 87 to 33% as the reduction temperature increases to 662°C in the presence of H_2. This is accompanied by a corresponding increase in the abundance of Component B over the temperature range studied.

DISCUSSION

Factor analysis of the V $2p_{3/2}$ spectra indicated that two components are present in the spectra of reduced V/Al_2O_3 catalyst when either H_2 or CO is used as the reducing agent. The position of component A from FA and NLLSCF (517.2 ± 0.2 eV) agrees well with the V $2p_{3/2}$ binding energy we have measured for V_2O_5 and NH_4VO_3 (517.2 eV). Furthermore, in the oxidic catalyst, V is expected to be in the highest oxidation state (+5); thus we assign Component A to the V^{5+} oxidation state.

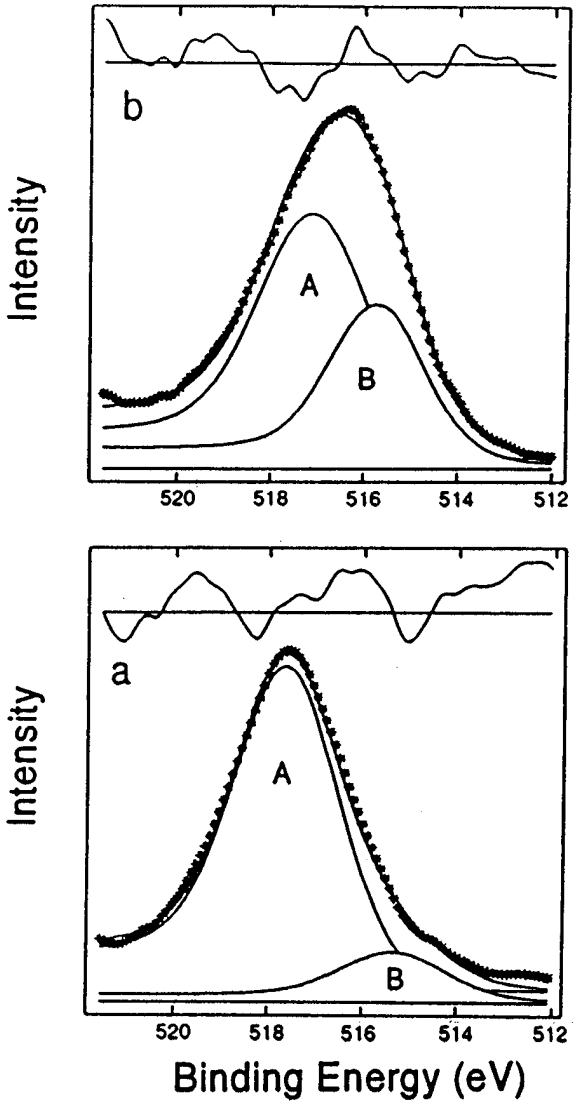

FIG. 5. V $2p_{3/2}$ envelopes curve fitted with components A (517.1 eV) and B (515.6 eV). (a) Oxidic V/Al_2O_3; (b) V/Al_2O_3 reduced in H_2 at 312°C. The residuals, shown at the top of each spectrum, indicate the difference between the fit and the original spectrum.

Because of the wide variation in the reported binding energies for all V oxidation states, Component B and Component C (515.5 and 515.8 eV) cannot be readily assigned to a specific oxidation state based solely on peak positions. We examined the *difference* in the binding energies, Δ_{BE}, of V^{5+} and lower oxidation states. Table 3 summarizes the Δ_{BE} of model V compounds from the present study and the literature. In general, the Δ_{BE} between V^{5+} and V^{4+} is 1.0 eV and the Δ_{BE} between V^{5+} and V^{3+} is ca. 1.5 eV. Recalling that the Δ_{BE}'s of Components A and B and A and C determined by factor analysis are 1.7 and 1.5 eV from H_2 and CO reduction, respectively, we can tentatively assign both Components B and C to V^{3+}. The XPS results are consistent with a recent study of model V/Al_2O_3 catalysts

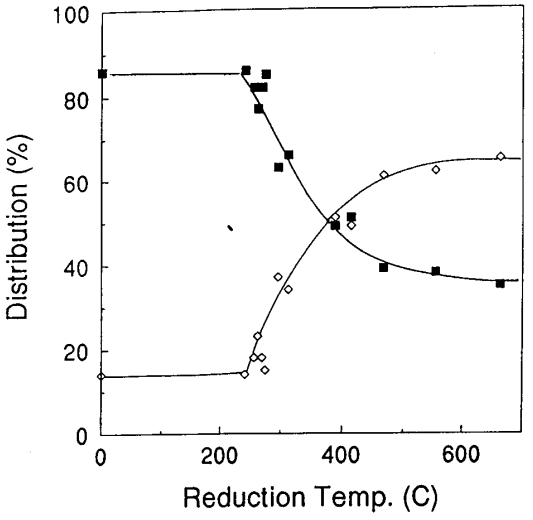

FIG. 6. Distribution of components A (■) and B (◇) from curve fitting the V $2p_{3/2}$ spectra of samples reduced in H_2.

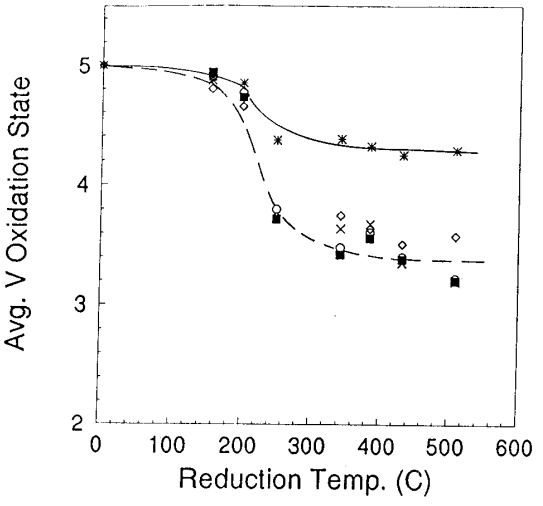

FIG. 7. Average V oxidation state of the catalyst after reduction in CO, estimated from: CO consumption (■), CO_2 formation (X), O_2 consumption on reoxidation (○), curve fitting the XPS V $2p_{3/2}$ spectra assuming component C is V^{3+} (◇), curve fitting the XPS V $2p_{3/2}$ spectra assuming component C is V^{4+} (*). See text for details.

(V/Al_2O_3 on Au coated Si(100 wafers) (28), where a binding energy shift of 1.5 eV observed on reduction at 450°C was attributed to V^{3+} formation.

Additional evidence for the assignment of the lower oxidation state to V^{3+} was sought from comparison of the average V oxidation state measured volumetrically with that estimated from XPS. Figure 7 shows the average V oxidation state obtained from CO consumed, from CO_2 formed, and from O_2 uptake upon reoxidation. The average oxidation state decreased from 5 to 3.3 as the reduction temperature was increased from 150 to 510°C. Figure 7 also shows the average oxidation state calculated from the curve-fitted spectra of the CO-reduced samples, assuming that Component C is V^{4+} or V^{3+}. It is clear that a better agreement with the volumetric measurements is obtained when Component C is assigned to V^{3+} (an average V oxidation state of 3.6 is measured on reduction at 510°C vs 4.3 if Component C is assigned to V^{4+}). Thus the volumetric study supports the initial assignment of Components B and C to V^{3+}. Based on this assignment one can calculate from Fig. 6 the V average oxidation state for the catalyst reduced in H_2. Note that for both CO and H_2 reduction, the values derived from XPS were corrected for sintering of the reduced species (see Eqs. [1] and [2]) and for the reduction occurring in the XPS chamber. The results shown in Fig. 8 indicate that the V average oxidation state decreases from 5 to 3.5 upon increasing the reduction temperature up to 662°C. The results of the present study are in agreement with those reported by Stopka and Cizek (12), where an average oxidation state of ca. 3.3 for V/Al_2O_3 reduced in H_2 at 450°C was measured by chemical analysis. The present results are also comparable with TPR results, which indicate that ca. 1 oxygen atom is removed per vanadium, indicating $V^{5+} \rightarrow V^{3+}$ (8).

Factor analysis and curve-fitting results show that reduction of the V phase proceeds from +5 to +3. No evidence for V^{4+} formation was found. The intermediate oxidation state V^{4+} has been detected by previous ESR studies of V/Al_2O_3 catalysts (12–15). However, the fraction of V^{4+} present after H_2 reduction was not reported (12, 15). In addition, our preliminary ESR examination of the reduced catalyst showed no appreciable amount of V^{4+}. Although the present study could detect only V^{5+} and V^{3+} in reduced catalyst, this does not rule out the possibility that a small amount of V^{4+} is present, which could be missed by FA. Under both H_2 and CO reducing conditions, the average

TABLE 3

V $2p_{3/2}$ Binding Energy Differences for Model Compounds and V/Al_2O_3 Catalyst

Δ_{BE} [V^{5+}–V^{4+}] (eV)	Δ_{BE} [V^{5+}–V^{3+}] (eV)	Reference this work
1.1		
0.7	1.5	(11)
0.9	1.5	(39)
1.0	1.2	(21, 29)
0.7	1.2	(17)
0.3		(24)
1.1	2.0	(40)
0.9		(26)
	1.9	(27)
1.0	1.4	(23)
1.0		(22)
	1.5	(28)
	1.7	This work (H_2 reduction)
	1.5	This work (CO reduction)

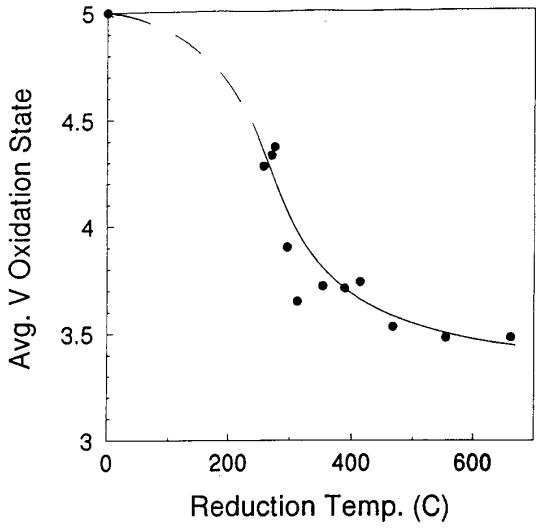

FIG. 8. Average V oxidation state of the catalyst after reduction in H_2, estimated by curve fitting the XPS V $2p_{3/2}$ spectra. See text for details.

oxidation state decreases rapidly after the onset of reduction (Figs. 7 and 8). This limits the range of temperatures in which V^{4+} may be present in a significant amount. If the V^{4+} is quickly reduced to a lower oxidation state, its contribution to the V 2*p* envelope will be small and may occur in only one or two spectra of the series. This, combined with a peak separation that is smaller than that generally reported between V^{5+} and V^{4+}, may prevent FA from detecting a small amount, <5% (35), of V^{4+} if present.

CONCLUSION

PCA and ITTFA were performed on a series of reduced 5.9 wt% V/Al_2O_3 catalyst to determine the number, position, and FWHMs of the spectral components, or oxidation states, which are present in the V 2*p* region. All statistical measures indicate the presence of two oxidation states, when either H_2 or CO is used as the reducing agent. ITTFA showed real spectral components at 517.2 and 515.5 eV for catalyst reduced in H_2 and at 517.3 and 515.8 eV for CO-reduced samples. The spectral information (position, FWHM, and number of components) derived from purely statistical means was used to curve fit the XPS V 2*p* region of the reduced catalyst and to obtain the distribution of V oxidation states. Based on the chemical shift of the V $2p_{3/2}$ peak and the stoichiometric reduction of V in CO, the two spectral components were assigned to V^{5+} and V^{3+}. The extent of reduction of the V phase was estimated from the relative abundances of V^{5+} and V^{3+} determined by curve fitting and corrected for the presumably lower dispersion of the V^{3+} species. The results indicated a decrease in the average oxidation state of V to 3.5 with increase of the reduction temperature in H_2 up to 662°C. When CO was used as the reducing agent, the average oxidation state decreased from 5 to 3.6 as the reduction temperature increased from 155 to 510°C.

ACKNOWLEDGMENTS

This work was supported by the National Science Foundation Grant CHE-9022135 and the Materials Research Center with funding from the Air Force Office of Scientific Research.

REFERENCES

1. Bond, G. C., and Tahir, S. F., *Appl. Catal.* **71**, 1 (1991).
2. Bonnelle, J. P., Derouane, E., and Delmon, B., Eds. "Surface Properties and Catalysis by Non-metals." Reidel, Dordrecht, 1983.
3. Andrews, A., Bovin, J. O., and Walter, P., *J. Catal.* **98**, 204 (1986).
4. Sanati, M., and Andersson, A., *J. Mol. Catal.* **59**, 233 (1990).
5. Roozeboom, F., Cordingley, P. D., and Gellings, P. J., *J. Catal.* **68**, 464 (1981).
6. Deo, G., and Wachs, I. E., *J. Catal.* **129**, 307 (1991).
7. Koranne, M. M., Goodwin, Jr., J. G., and Marcelin, G., *J. Catal.* **148**, 369 (1994).
8. Roozeboom, F., Mittelmeijer-Hazeleger, M. C., Moulijn, J. A., Medema., J., and de Beer, V. H. J., *J. Phys. Chem.* **84**, 2783 (1980).
9. Harber, J., Kozlowska, A., and Kozlowski, R., *J. Catal.* **102**, 52 (1986).
10. Roozeboom, F., van Dillen, A. J., Geus, J. W., and Gellings, P. J., *Ind. Eng. Chem. Prod. Res. Dev.* **20**, 304 (1981).
11. Nag, N. K., and Massoth, F. E., *J. Catal.* **124**, 127 (1990).
12. Stopka, P., and Cizek, M., *Collect. Czech. Comm.* **57**, 1023 (1992).
13. Inomata, M., Mori, K., Miyamoto, A., and Murakami, Y., *J. Phys. Chem.* **87**, 761 (1983).
14. Yoshida, S., lguchi, T., Ishida, S., and Tarama, K., *Bull. Chem. Soc. Jpn.* **5**, 376 (1972).
15. Chary, K. V. R., Mahipal Reddy, B., Nag, N. K., Subrahmanyam, V. S., and Sumandana, C. S., *J. Phys. Chem.* **88**, 2622 (1984).
16. Wertz, J. E., and Bolton, J. R., Eds., "Electron Spin Resonance: Elementary Theory and Practical Applications." Chapman & Hall, New York, 1986.
17. Sawatzky, G. A., and Post, D., *Phys. Rev. B* **20**, 1546 (1979).
18. Gil-Llambias, F. J., Escudey, A. M., Fierro, J. L. G., and Lopez Agudo, A., *J. Catal.* **95**, 520 (1985).
19. Meunier, G., Mocaer, B., Kasztelan, S., LeCoustumer, L. R., Grimblot, J., and Bonnelle, J. P., *Appl. Catal.* **21**, 329 (1986).
20. Horvath, B., Strutz, J., Geyer-Lippmann, J., and Horvath, E. G., *Z. Anorg. Allg. Chem.* **483**, 181 (1981).
21. Andersson, S. L. T., *J. Chem. Soc., Faraday Trans. 1* **75**, 1356 (1979).
22. Chiarello, G., Robba, D., DeMichele, G., and Parmigiani, F., *Appl. Surf. Sci.* **64**, 91 (1993).
23. Rao, C. N. R., Sarma, D. D., Vasudevan, S., and Hedge, M. S., *Proc. R. Soc. London A* **367**, 239 (1979).
24. Kasperkiewicz, J., Kovacich, J. A., and Lightman, D., *J. Electron Spectrosc. Relat. Phenom.* **32**, 123 (1983).
25. Andersson, S. L. T., *Catal. Lett.* **7**, 351 (1990).
26. Jagannathan, K., Srinivasam, A., and Rao, C. N. R., *J. Catal.* **69**, 418 (1981).
27. Haber, J., Machej, T., and Czeppe, T., *Surf. Sci.* **151**, 301 (1985).
28. Nickl, J., Schild, Ch., Baiker, A., Hund, M., and Woukam, A., *Fresenius' J. Anal. Chem.* **346**, 79 (1993).
29. Odriozola, J. A., Soria, J., Somorjai, G. A., Heinemann, H., Garcia de la Banda, J. F., Lopez Granados, M., and Conesa, J. C., *J. Phys. Chem.* **95**, 240 (1991).
30. Nogier, J. P., Jammul, N., and Delamar, M., *J. Electron Spectrosc. Relat. Phenom.* **56**, 279 (1991).

31. Proctor, A., and., Hercules, D. M., *Appl. Spectrosc.* **38**, 505 (1984).
32. Fiedor, J. N., Proctor, A., Houalla, M., and Hercules, D. M., *Surf. Interface Anal.* **20**, 1 (1993).
33. Stranick, M. A., Houalla, M., and Hercules, D. M., *J. Catal.* **103**, 151 (1987).
34. Kerkhof, F. P. J. M., and Moulijn, J. A., *J. Phys. Chem*. **83**, 1612 (1979).
35. Scierka, S. J., Proctor, A., Houalla, M., and Hercules, D. M., *Surf. Interface Anal.* **20**, 901 (1993).
36. Malinowski, E. R., "Factor Analysis in Chemistry." Wiley, New York, 1991.
37. Malinowski, E. R., *J. Chemom*. **3**, 49 (1988).
38. Reinsch, C. R., *Numer. Math*. **10**, 177 (1967).
39. Colton, R. J., Guzman, A. M., and Rabalais, J. W., *Acc. Chem. Res.* **11**, 170 (1978).
40. Hamrin, K., Nordling, C., and Kihlborg, L., *Ann. Acad. Regiae. Sci. Upsal.* **14**, 70 (1970).